

# Distortion of Magnetic Resonance Images and Treatment Planning for Stereotactic Radiosurgery

Shin IKEDA<sup>1</sup>, Masahiro MORIYAMA<sup>1</sup>, Masaki YOKOKAWA<sup>1</sup>, Atsuya KAWAGUCHI<sup>1</sup>,  
Koji UCHIDA<sup>2</sup>, Hajime KITAGAKI<sup>2</sup> and Nobue UCHIDA<sup>1</sup>

<sup>1</sup>*Department of Radiation Oncology, Shimane University Faculty of Medicine (89-1, Enya, Izumo, Shimane 693-8501, Japan)*

<sup>2</sup>*Department of Radiology, Shimane University Faculty of Medicine (89-1, Enya, Izumo, Shimane 693-8501, Japan)*

(Received July 21, 2011; Accepted November 7, 2011)

While CT is essential for planning radiation therapy, MRI is used for imaging brain tumors for greater soft tissue contrast and more accurate depiction of tumors, particularly in cases involving stereotactic radiosurgery (SRS). However, MRI is characterized by greater image distortion than CT, making accurate localization of the target tumor difficult. This study evaluated the effects of such distortion on SRS planning. CT and MRI incorporating SRS planning parameters were performed on a brain phantom, and the images were then fused for comparison. We compared treatment parameters obtained from CT data alone with those obtained from the fused images. A maximum linear distortion of 3.3 mm was observed on coronal MRI. When SRS planning incorporated the coronal MRI data, treatment parameters derived from CT data alone were less accurate than those obtained from the fused images.

---

Key words: stereotactic radiosurgery / magnetic resonance imaging / distortion / radiation therapy planning / image fusion

## INTRODUCTION

Stereotactic radiosurgery (SRS) has recently become more widely used for metastatic brain tumors. Multidisciplinary therapy, such as the combination of whole brain irradiation with SRS or surgery, achieves superior results in terms of survival, neu-

rocognitive function, and quality of life [1]. In contrast, the clinical benefit and optimal regimen for chemotherapy and radiosensitizing agents remain unclear in treatment of metastatic brain tumors [2].

Radiation oncologists commonly use computed tomography (CT), as it provides data on X-ray absorption. Magnetic resonance imaging (MRI) achieves greater soft tissue contrast and a more accurate depiction of a tumor than does CT, but provides no information on X-ray absorption. Therefore, fused MRI/CT images are now used clinically [3]. Gadolinium-enhanced 3-dimension gradient echo (3D-GRE) images are used for fusion purposes because of their high resolution, short acquisition time, and T1-weighted contrast [4, 5]. However, 3D GRE images have greater distortion than spin echo images due to nonlinearity of the gradient field, inhomogeneity of the magnetic field related to the eddy current, magnetic susceptibility, and the distance from the field isocenter [3, 6]. Distortion is also affected by the magnetostatic strength [7]. To our knowledge, there have been no studies on the influence of distortion of MRI (3D-GRE) images on dose delivery in cases of SRS. Accordingly, we investigated the influence on localization of the distortion on MR images in a comparison with CT scans relative to the special SRS frame, and the influence on radiation therapy planning, using a brain phantom.

## MATERIALS AND METHODS

### *Brain phantom*

A phantom was created having T1 & T2 values similar to those of brain tissue, as previously described [8, 9]. A mixture of 3.0% carrageenan

---

Correspondence: Shin Ikeda  
89-1 Enya, Izumo, Shimane 693-8501, Japan  
Tel:+81-853-20-2582  
Fax:+81-853-20-2582  
Email:ikedashin7777@gmail.com

gel, 60  $\mu\text{mol/kg}$  gadodiamide hydrate, 1.0% agarose gel, 0.24% NaCl, 0.03%  $\text{NaN}_3$ , and distilled water (2000 ml) was gradually heated while stirring until boiling and then poured into a pair of hemispherical molds (15 cm in diameter). Three “tumors” composed of butadiene resin were also prepared: one sphere approximately 3 cm in diameter and two sphere approximately 2 cm in diameter. These were randomly placed in the peripheral area of the cooling phantom to represent tumors. After the molded forms cooled, the two hemispheres were joined together to make the brain phantom (Figs. 1 and 2). Three small titanium cylinders (4.5 mm

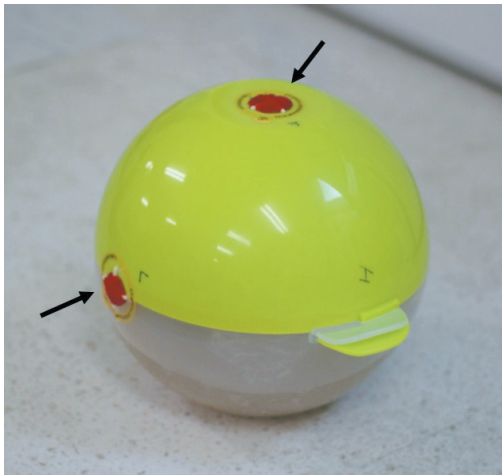


Fig. 1. Appearance of the phantom: The phantom is made of carrageenan gel covered with plastic, and scan reference markers covered with red clay are attached (arrow).

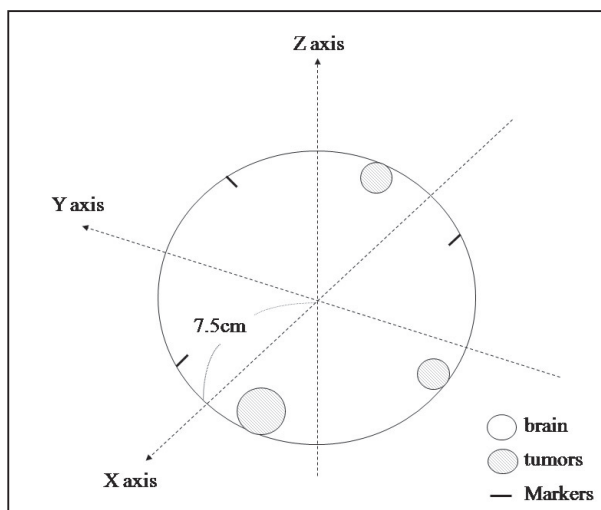


Fig. 2. Diagram of the brain phantom and tumor phantoms. The radius of the brain phantom is approx. 7.5 cm. The larger “tumor” is approx. 3 cm diameter and the two smaller “tumors” approx. 2 cm diameter.

length and 0.8 mm in diameter) or inactive dummy sources for low-dose rate brachytherapy were implanted as markers, for purposes of identifying a high-density metal structure on the CT scans and as a signal void on the MR images.

### Fixation and treatment planning

The Brain SCAN frame (Brain LAB AG<sup>®</sup>; BrainLAB AGKapellenstr. 12, 85622 Feldkirchen, Germany) was used to fix the phantom. Radiation therapy was planned with Brain SCAN software (ver. 5.31 Build 234) (Brain LAB AG<sup>®</sup>).

### Image acquisition

A three-axis laser pointer was used to set the position of the phantom, and the phantom was fixed in a craniocaudal, right-left, or anteroposterior direction. The origin point (the scan reference point) was marked by set-up markers that did not cause artifacts. The phantom was set up for MRI in the same manner, but the set-up markers were covered with clay, otherwise the markers would have no magnetic resonance signal (Figs. 1, 3 and 4). The CT scan reference point was confirmed and set at the magnetic field isocenter. The planes of the three landmarks were not parallel to the 3 MR axes. The parameters for image acquisition are shown in Tables 1 and 2.

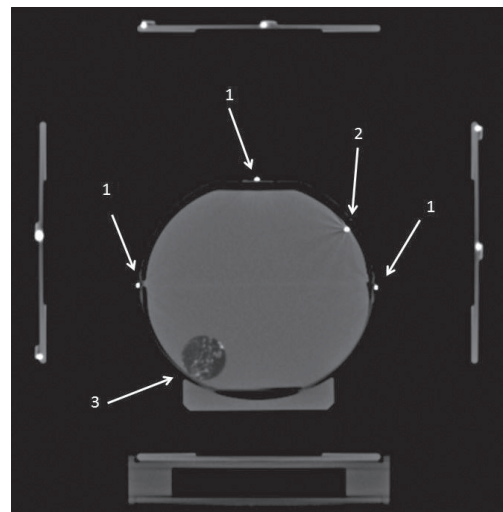


Fig. 3. CT scan of the phantom, stereotactic frame, set-up markers (Window width 1400, window center 300). 1: scan reference markers, 2: titanium marker, 3: tumor phantom. Other objects are parts of Brain scan frame.

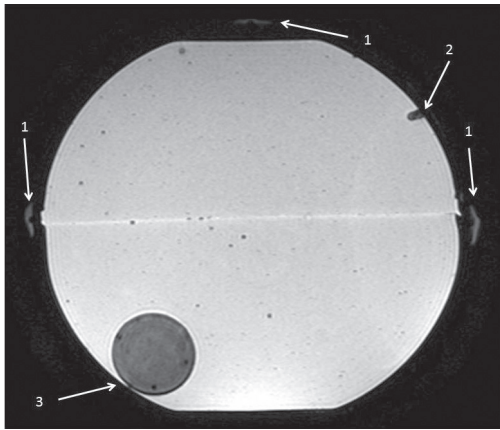


Fig. 4. MR image of the phantom; set-up markers showed as signal void (Window width 8000, window center 4000). 1: scan reference markers, 2: titanium marker, 3: tumor phantom.

Table 1. Parameters for acquisition of CT scans

CTscanner:Sensation24(Siemens) Parameters	
Tube voltage	120 kV
Tube current	320 mA
Collimation	1.2 mm×24
Slice thickness	1.5 mm
Slice interval	0 mm
Matrix	512×512
FOV	370×370

Table 2. Parameters for acquisition of MR images

MRI unit: Signa HDx 3.0T (GE Medical Systems) Parameters	
Image mode	3-dimensional
Encoding	fast SPGR
Repetition time	6.8 msec
Echo time	2.0 msec
Inversion time	700 msec
Flip angle	12°
Matrix size	512×256
Voxel size	0.86×0.86×1.6 mm
FOV	220 mm
Slice plane	Axial, coronal, sagittal

### Image fusion

Fusion Viewer 2.0 software (Nihon Medi-physics<sup>®</sup>; 3-4-10, Shinsuna, Koto-ku, 136-0075 Tokyo, Japan) was employed for fusion of the CT scans with the MR images. Because it is necessary to eliminate individual differences of the image fusion systems, and automatic fusion is often not accurate enough, the fusion was performed manually.

CT scans were fused with each of 3 sets of MR images (axial, coronal, and sagittal images) using the three titanium cylinders as landmarks. If there were no distortion, the 3 axes and 3 landmarks



Fig. 5. Image (c) was created by manual fusion of an MR image (a) and a CT scan (b) using software. Distortion of the fused image is obvious, even when the 3 spatial landmarks are matched.

would match precisely, as would the pair of 3-D images. However, distortion affects not only the tumor but also the phantom and markers on MR images, making impossible precise fusion of CT and MR data. Therefore, image fusion was performed manually by five radiation oncologists to achieve the best possible outcome (Figs. 5a-c).

### Measurement of distortion

We measured the greatest displacement of the phantom tumor on the fused images (Fig. 6) by counting pixels between the tumor contours of the compared MRI data and CT scans. As the base of the SRS frame is 100 mm in length, the absolute distortion could be estimated based on the ratio of the number of pixels. Images were viewed with an “SDS viewer” (Version 4.3.14, Tecmatrix Japan<sup>®</sup>4-10-8, Takawawa, Shinagawa, 108-8588 Tokyo, Japan.).



Fig. 6. Measuring linear distortion of the fused image. The greatest distance between the contours of CT scans and MRI was measured, as described in Materials and Methods.

### SRS planning

After fusing the CT and MR images in the radiation therapy planning system, we planned the photon beams for SRS based on MRI tumor contours. The peripheral dose was 16 Gy delivered by 5 beam arcs with a circular collimator. Then we compared treatment parameters (maximum dose, minimum dose, and homogeneity index) based on CT and MRI tumor contours using the set of MR images with the greatest distortion.

## RESULTS

The CT scans and MR images were all of high

quality, with the landmarks for image fusion easily recognizable, as were the phantom tumors. With MRI, tumor outlines were sharper and clearer than with CT. Tumor location and size on CT did not match well with those on MRI with manual tumor contouring. The maximum linear distortion of the larger (3cm) tumor phantom outline was 3.3 mm (Fig. 6) when coronal MR images of this tumor were employed for fusion (1.5 mm with sagittal images and 3.2 mm with axial images) (Table 3). The smaller (2cm) tumor phantoms showed less than 2 mm distortion on each MR image. The tumor volume on coronal MR images was 12.75 cm<sup>3</sup>, approximately 10% smaller than shown on CT scans (14.18 cm<sup>3</sup>).

SRS planning with fused images derived from coronal MR images achieved worse radiation dosimetry and treatment parameters than those obtained with CT scans (Table 4, Fig. 7). The maximum dose was the same, but the peripheral minimum dose decreased from 16.2 Gy for the MRI tumor contour (>80% of the prescription dose) to 10.6 Gy for the tumor CT contour (only about 50% of the prescription dose). Dose volume histograms showed apparent deterioration of treatment quality for the CT tumor contour (Figs. 8a and 8b).

Table 3. Maximum linear distortion when each type of MR image was fused with CT scans

Slice plane	MD* (mm)
Axial	3.2
Sagittal	1.5
Coronal	3.3

\*MD: maximum displacement

Table 4. Comparison of therapeutic parameters for CT contour with MRI contour

	MRI (reference)	CT (true)
Maximum dose	25.6 Gy	25.6 Gy
Minimum dose	16.2 Gy	10.6 Gy
Homogeneity index	158%	242%
Volume of the contour	12.75 ml	14.18 ml

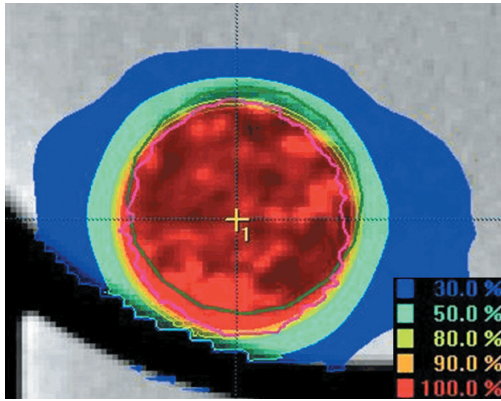


Fig. 7. SRS planning with MRI. The CT contour is green and the MRI contour is pink. Because we used a coronal MR image, the contour that we designed manually is wavy-like due to distortion. The peripheral dose is inadequate compared with that obtained by SRS planning with CT.

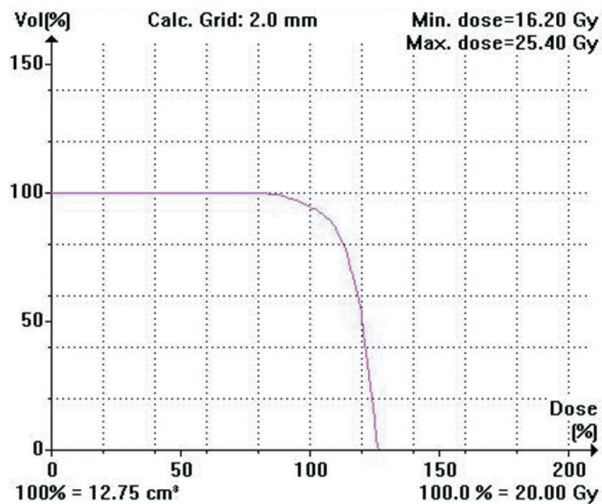


Fig. 8a. DVH of MR images shows an adequately sharp curve.

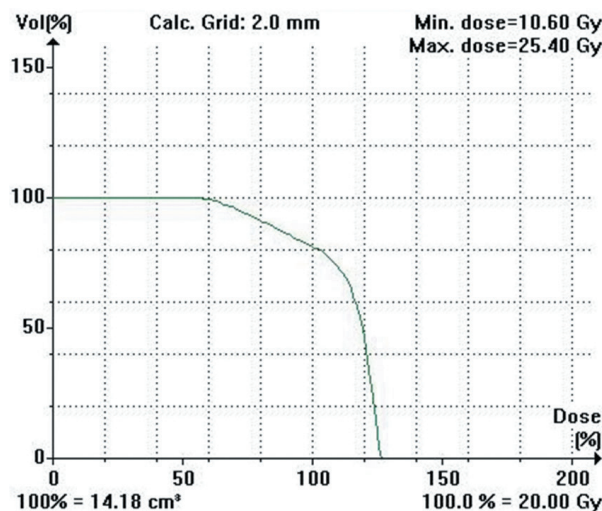


Fig. 8b. DVH of CT scans shows an inadequate curve.

## DISCUSSION

Spatial information and electron density data obtained from CT scans are essential for radiosurgery with a linear accelerator (linac surgery), as the CT tumor contour helps to determine the true gross tumor target volume (GTV). However, evaluation of the GTV on plain CT scans is difficult due to poor tissue contrast, especially in the case of brain lesions. Even with contrast enhancement, the GTV remains unclear on CT [10], so planning SRS with CT alone is problematic. CT images are also influenced by beam-hardening artifacts caused by the skull bone or exogenous metal components. MRI achieves better tissue contrast, especially with brain tumors; thus an MRI-depicted tumor contour is very helpful in determining the reference GTV. In general, radiation oncologists now use fused images utilizing both CT and MRI data for SRS planning in clinical practice.

However, it is widely acknowledged that image distortion in MRI creates discrepancies in brain images. On fused CT and MRI images, even with the alignment of three spatial position landmarks with laser pointer markers for set-up, the inaccuracy of MRI data persists due to image distortion, posing a significant problem to SRS planning.

Linear distortion of MR images, regardless of technical and experimental parameters, reportedly ranges from <1 mm to >10 mm, though predominantly in the range of 2-3 mm, particularly along the cranio-caudal axis [7, 11-18]. While image distortion in gamma knife surgery for SRS has been evaluated, its effect on linac surgery has yet to be fully evaluated due to the newness of the technique [7].

Although high-resolution T1 3D-GRE images are useful in defining the tumor contour, the linear distortion ranges from 0.5 to 2 mm [18]. The present study shows that linear distortion of as much as 3.3 mm in MR coronal images can occur in peripheral regions of the brain. This result cannot be overlooked in light of the need for accuracy of measurements in linac surgery of within approximately 1 mm.

In SRS planning, 1-2mm is added to GTV as a tumor margin [19]. This added margin is not to compensate for imaging discrepancies, but rather

is solely as an allowance for set-up error. Because minimum dose, prescription dose, and tumor volume are critical factors in SRS [20], these parameters must be defined accurately. Generally, a minimum dose for metastatic brain tumors should be >12 Gy and the prescription dose >14 Gy [20]. It is possible the peripheral region of a brain tumor may lie outside the MRI-delineated contour, as our phantom study showed a 3 mm gap between CT and MRI tumor contours at 7.5 cm from the center of the magnet. Therefore, such distortion on the MR image may prevent local control and lead to more frequent recurrences or residual tumors due to inadequate coverage and dose levels in the course of SRS. This may serve to explain why larger tumors show lower rates of local control after SRS, as such tumors have a proportionately greater peripheral zone volume than smaller tumors. In the present study, the radiation therapy planning system achieved worse SRS parameters (peripheral minimum dose and homogeneity index) with the CT tumor contour (true target tumor) than with the MRI tumor contour (reference target tumor).

As the irradiated volume increases in SRS, so do the adverse effects [19, 21], including brain necrosis and atrophy. Radiation treatment planning without an adequate margin (to lower the risk of adverse effects), or without consideration of MR image distortion of tumor contours, may lead to a worse outcome, especially in patients with larger tumors.

In this phantom experiment, it was possible to distinguish the tumor outline on plain CT scans, and to identify discrepancies between CT and MRI-depicted tumor contours. However, as it is not possible to clearly delineate a brain tumor on plain CT scans obtained from patients for purposes of treatment planning, the quality of the fused CT scan and MR image must be ensured in various ways during SRS planning. As well as matching structures such as bones, eyeballs, and ventricles, there should also be an attempt to match normal sulci and gyri close to the tumor. In addition, CT and MRI data for each tumor should be separately fused if multiple metastatic tumors are irradiated after a single set-up, and planning should not be exclusively based on an automatic fusion system without

additional verification. In this study, the distortion of MR images was evaluated linearly by verifying the positions of markers.

Regardless of efforts to minimize the influence of distortion at the time of image acquisition, some distortion will remain on the MR image. The inability to determine or recognize the extent of such distortion in a clinical setting has been a significant problem for radiation oncologists. This study used a brain phantom with artificial tumors which were well-defined on both plain CT and MRI, and permitted the evaluation of the influence of accuracy on treatment planning. The nature and extent of any such influence in an actual clinical setting is a matter of speculation and future study.

In conclusion, this study showed that image distortion on MRI may significantly influence the outline of the target and estimated tumor volume, as well as the dosage delivered to the tumor.

## ACKNOWLEDGEMENTS

We thank Mr. Nishimura of the Department of Radiology, Shimane University Hospital, for his help with collecting and analyzing data for this study. A part of this study was supported by a Grant-in-aid for medical scientific research from Shimane University Hospital, Japan.

## REFERENCES

- 1) Rades D, Kueter JD, Hornung D, Veninga T, Hanssens P, Schild SE and Dunst J (2008) Comparison of stereotactic radiosurgery (SRS) alone and whole brain radiotherapy (WBRT) plus a stereotactic boost (WBRT SRS) for one to three brain metastases. *Strahlenther Onkol* 184: 655-662
- 2) Ranjan T and Lauren EA (2009) Current management of metastatic brain disease. *Neurotherapeutics* 6: 598-603
- 3) Khoo VS and Joon DL (2006) New developments in MRI for target volume delineation in radiotherapy. *Br J Radiol* 79 Spec No 1: 2-15
- 4) Kristensen BH, Finn JL, Vibeke L, Poul FG and Anders KH (2008) Dosimetric and geometric evaluation of an open low-field magnetic

- resonance simulator for radiotherapy treatment planning of brain tumours. *Radiother Oncol* 87: 100-109
- 5) Engh JA, John CF, Niranjana A, Devin VA, Douglas SK and Lunsford LD (2007) Optimizing intracranial metastasis detection for stereotactic radiosurgery. *Stereotact Funct Neurosurg* 85: 162-168
  - 6) Moore CS, Gary PL and Andrew WB (2004) Quality assurance of registration of CT and MRI data sets for treatment planning of radiotherapy for head and neck cancers. *J Appl Clin Med Phys* 5: 25-35
  - 7) Watanabe Y, Chung KL and Bruce JG. (2006) Geometrical accuracy of a 3-tesla magnetic resonance imaging unit in Gamma Knife surgery. *J Neurosurg* 105 Suppl: 190-193
  - 8) Yoshimura K, Kato H, Kuroda M, Yoshida A, Hanamoto K, Tanaka A, Tsunoda M, Kanazawa S, Shibuya K, Kawasaki S and Hiraki Y (2003) Development of a tissue-equivalent MRI phantom using carrageenan gel. *Magn Reson Med* 50: 1011-1017
  - 9) Oonishi H (2004) Tissue contrast, some clinical applications. In: *MRI The Basics Second Japanese Edition*. (Hashime RH., Bradley WG and Lisanti CJ., ed.) pp. 62, Medical science international, Tokyo
  - 10) Sidhu K, Cooper P, Ramani R, Schwartz M, Franssen E and Davey P (2004) Delineation of brain metastases on CT images for planning radiosurgery: concerns regarding accuracy. *Br J Radiol* 77: 39-42
  - 11) Prabhakar R, Julka PK, Ganesh T, Munshi A, Joshi RC and Rath GK (2007) Feasibility of using MRI alone for 3D radiation treatment planning in brain tumors. *Jpn J Clin Oncol* 37: 405-411
  - 12) Wyper DJ, Turner JW, Patterson J, Condon BR, Grossart KWM, Jenkins A, Hadley DM and Rowan JO (1986) Accuracy of stereotaxic localisation using MRI and CT. *J Neurol Neurosurg Psychiatr* 49: 1445-1448
  - 13) Burchiel KJ, Nguyen TT, Coombs BD and Szumoski J (1996) MRI distortion and stereotactic neurosurgery using the Cosman-Roberts-Wells and Leksell frames. *Stereotact Funct Neurosurg* 66: 123-136
  - 14) Webster GJ, Kilgallon JE, Ho KF, Rowbottom CG, Slevin NJ and Mackay RI (2009) A novel imaging technique for fusion of high-quality immobilised MR images of the head and neck with CT scans for radiotherapy target delineation. *Br J Radiol* 82: 497-503
  - 15) Yu C, Apuzzo ML, Zee CS and Petrovich Z (2001) A phantom study of the geometric accuracy of computed tomographic and magnetic resonance imaging stereotactic localization with the Leksell stereotactic system. *Neurosurgery* 48: 1092-1098
  - 16) Chen L, Price RA Jr, Wang L, Li J, Qin L, McNeeley S, Ma CM, Freedman GM and Pollack A (2004) MRI-based treatment planning for radiotherapy: dosimetric verification for prostate IMRT. *Int J Radiat Oncol Biol Phys* 60: 636-647
  - 17) Landi A, Marina R, DeGrandi C, Crespi A, Montanari G, Sganzerla EP and Gaini SM (2001) Accuracy of stereotactic localisation with magnetic resonance compared to CT scan: experimental findings. *Acta Neurochir* 143: 593-601
  - 18) Veninga T, Huisman H, Richard WM and Huizenga H (2004) Clinical validation of the normalized mutual information method for registration of CT and MR images in radiotherapy of brain tumors. *J Appl Clin Med Phys* 5: 66-79
  - 19) Nataf F, Schlienger M, Liu Z, Foulquier JN, Grès B, Orthuon A, Vannetzel JM, Escudier B, Meder JF, Roux FX and Touboul E (2008) Radiosurgery with or without a 2-mm margin for 93 single brain metastases. *Int J Radiat Oncol Biol Phys* 70: 766-772
  - 20) Schomas DA, Roeske JC, MacDonald RL, Sweeney PJ, Mehta N and Mundt AJ (2005) Predictors of tumor control in patients treated with linac-based stereotactic radiosurgery for metastatic disease to the brain. *Am J Clin Oncol* 28: 180-187
  - 21) Chang EL, Wefel JS, Maor MH, Hassenbusch SJ 3rd, Mahajan A, Lang FF, Woo SY, Mathews LA, Allen PK, Shiu AS and Meyers CA (2007) A pilot study of neurocognitive function in patients with one to three new brain metastases initially treated with stereotactic radiosurgery alone. *Neurosurgery* 60: 277-283

